

STRUCTURAL TUNING THROUGH EMBEDDED ANGULAR MOMENTUM

Mason A. Peck

Member AIAA, Senior Staff Engineer, Honeywell Space Systems, Glendale, Arizona

Andrew R. Cavender

Project Engineer, Honeywell Space Systems, Glendale, Arizona

We propose a simple, yet versatile, concept for adaptive tuning of structural dynamics: embedding angular momentum in the structure to achieve such goals as frequency shifting, modal coupling or decoupling, and phase adjustment for the open-loop plant. We explore the theoretical aspects of this problem with a comparatively simple three-axis analytical model that includes a single embedded-momentum vector. A discussion of systems-engineering issues suggests that in cases of practical interest selecting a constant value for the angular momentum (on the basis of desired modal characteristics) can be sufficient to correct for pre-launch modeling uncertainty and environmental effects; active wheel torquing is unnecessary. In practice, this technique is well suited to spacecraft appendages where a momentum wheel or a reaction wheel can be mounted. The practicality and mass savings of this approach are discussed.

INTRODUCTION

Structural adaptation provides a means to compensate for the difficulty inherent in predicting flexible behaviors of spacecraft. It is therefore not surprising that as demands on spacecraft payload performance increase, requiring larger (and typically lower-frequency) solar arrays and antenna structures but with ever tighter requirements on the accuracy of predicted structural response, more attention is being paid to the relief offered by adaptively tuning a structure's response after the spacecraft has been launched. This trend, a continual rise in the pervasiveness of flexible dynamics in space systems despite limited success in improving prediction methods, has been evident at least since the Explorer era, and it shows no signs of abating in years to come.

A method of structural adaptation that has received some attention during the past decade, but which has rarely been discussed in practical terms, is gyroscopic augmentation. The principle is based on the observation that embedded angular momentum, also known as gyricity, influences the mode shapes and frequencies of a linear dynamic system. While the dynamics of gyroelastic systems has received thorough theoretical treatment, even to the extent that subtleties of controllability and observability have been

addressed, its promise as a means of structural adaptation has been of secondary interest. One of the objectives of the present study is to rectify this omission by enumerating the uses of embedded momentum for structural adaptation and evaluating their practicality in the context of near-term momentum-control technologies. Another is to illustrate by a simple example that designing in embedded momentum offers benefits in areas of interest in the practice of spacecraft engineering.

This study begins with a review of some excellent work in the area of gyroelastic dynamical systems due primarily to G. M. T. D'Eleuterio, P. C. Hughes, and G. R. Heppler. Having introduced the fundamentals of gyroelastic dynamics, we outline a systems-engineering process—a collection of design considerations—that might motivate embedding momentum in structures. This discussion includes an assessment of the current state of the art in the design of small momentum actuators.

Early work in the dynamics and control of flexible spacecraft focused on spinning satellites¹. The reasons can be found in the inherent ability of a momentum-bias system to attenuate the effects of torque disturbances on attitude even in the absence of active control made spinning spacecraft an excellent design choice when active control and spaceworthy electronics were less mature than they are today. Much of this work has also informed efforts in rotordynamics (e.g. for helicopters), where stiffening due to the spin field and related effects have a profound influence on the system dynamics^{2,3,4}.

Probably the earliest work in the area of distributed gyricity—that is, angular momentum smeared across a structure as a continuum—appeared in G. M. T. D'Eleuterio's dissertation⁵ and his subsequent work^{6,7,8,9,10}. He and Hughes proposed the concept in the same spirit as continuous mass and stiffness distributions are sometimes used to represent large truss-like lattice structures¹¹. We follow their development, which uses Hamilton's Principle, with only minor departures. We begin by defining a the kinetic energy δT of a differential mass element $\sigma \delta V$:

$$\delta T = \frac{1}{2}(\mathbf{v} + \boldsymbol{\omega}_h \times \mathbf{r}_h) \cdot (\mathbf{v} + \boldsymbol{\omega}_h \times \mathbf{r}_h) \sigma \delta V, \quad (1)$$

where the vector \mathbf{v} is the translational velocity of the mass element, \mathbf{r}_h is the position of the mass element, fixed in a local frame, and $\boldsymbol{\omega}_h$ is the angular velocity of this body-fixed frame relative to an inertial frame. This vector expression yields a scalar; therefore, the choice of basis vectors with which to associate vector components is irrelevant. It has been claimed that the angular velocity $\boldsymbol{\omega}_h$ can be considered the sum of two parameters: the rotation of the element due to elastic deformation and an implicit angular velocity of the gyricity. One must be careful in making this simplification that the energy required to spin up or down the differential element of angular momentum is not of interest. If it is, as in the case of active control via gyric actuators, the choice of inertia for the differential gyricity element is not arbitrary, and instead there is an issue of core energy to be considered, as discussed elsewhere^{12,13}.

After integrating this differential element over the volume of the body, one finds that the equation of motion for a gyroelastic body in matrix-operator form is

$$M\ddot{\mathbf{u}} + G\dot{\mathbf{u}} + K\mathbf{u} = \mathbf{f} + \frac{1}{2}\nabla^\times g. \quad (2)$$

In this result, the mass matrix operator M is taken to depend only on the mass-density distribution σ so that

$$M = \sigma \mathbf{1}, \quad (3)$$

where $\mathbf{1}$ indicates the identity operator. Also, the rate-dependent forces arise from the operator

$$G = -\frac{1}{4}\nabla^\times h^\times \nabla^\times, \quad (4)$$

where the notation $^\times$ denotes the skew-symmetric matrix equivalent of the cross product operation; and thus ∇^\times is the curl operator. The stiffness operator K depends on a tensor of Young's moduli as discussed in D'Eleuterio⁸.

An analysis of the modal characteristics of this system leads to several important conclusions:

- Gyroelastic vehicles exhibit at least one mode whose frequency is zero but whose associated (elastic) strain energy is nonzero¹¹. In fact, these rigid-body deformed modes are six in number, not one, for a gyrostat¹³. In these modes, gyricity

causes deformation in the structure in steady state due to the constant, body-fixed torque imparted by the cross product of vehicle rate and the embedded momentum.

- The introduction of gyricity can be responsible for the appearance of complex-conjugate pairs of eigenvalues (and associated eigenvectors). These bifurcations are demonstrated in the example.
- The modal frequencies and shapes are gyricity dependent.

AN ILLUSTRATIVE EXAMPLE

We now consider a simple example to illustrate the concept explicitly. The objective is to demonstrate how the eigenvalues of the system change with gyricity, which can be accomplished in a closed form even in three dimensions with sufficient foresight in the construction of the example. A microsatellite with a single flexible appendage, such as a gimbaled optical instrument, provides our motivation. The satellite and its appendage dynamics are modeled as two rigid bodies connected by a three degree-of-freedom rotational stiffness matrix. The appendage is pinned to the central body, eliminating relative translation. The appendage is also given some embedded gyricity, shown here as a small momentum wheel whose inertia contributes to that of the appendage such that their total is completely spherical (all moments of inertia equal). For simplification the flexible body is taken to be rigid, and its mass center is taken to coincide with the attachment point. Furthermore, it is assumed to experience only small displacements relative to the spacecraft body. Figure 1 is a sketch of such a system. Figure 2 shows the appendage as a solid model with some explicit rotational springs and a momentum wheel.

We define a frame B fixed in the spacecraft body and an inertial (or Newtonian) frame N. Because the appendage is statically balanced—i.e., the pivot point coincides with its own mass center—the angular momentum \mathbf{H} for the mass center of such a system is

$$\mathbf{H} = \mathbf{I}_1 \cdot \boldsymbol{\omega}^{B/N} + \mathbf{I}_2 \cdot (\boldsymbol{\omega}^{A/B} + \boldsymbol{\omega}^{B/N}) + \mathbf{h} \quad (5)$$

where the superscripts N, A, and B indicate respectively the inertial frame, an appendage-fixed frame, and the body-fixed frame; \mathbf{I}_1 is the rigid body's inertia dyadic for the system mass center, including the transfer term due to the offset of the appendage's mass center from that of the system mass center, and \mathbf{I}_2 is the inertia dyadic of the appendage for its mass center; $\boldsymbol{\omega}^{B/N}$ is the

angular velocity of B in N, and $\omega^{A/B}$ is the angular velocity of appendage in B.

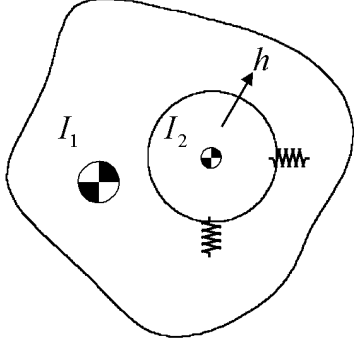


Figure 1. Sketch of the two-body system with appendage gyricity.

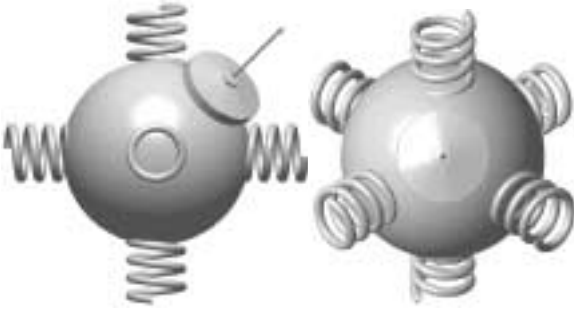


Figure 2. Two views of the spherical appendage with 3DOF stiffness and embedded gyricity.

The assumption that the appendage is statically balanced ensures that the system mass center remains fixed in B.

The rotational motion of the system of bodies is described by the vector equation

$$\begin{aligned} \frac{N}{dt} \mathbf{H} = & \mathbf{I}_1 \cdot \frac{B}{dt} \boldsymbol{\omega}^{B/N} + \mathbf{I}_2 \cdot \frac{B}{dt} (\boldsymbol{\omega}^{A/B} + \boldsymbol{\omega}^{B/N}) + \\ & \frac{B}{dt} \mathbf{h} + \boldsymbol{\omega}^{B/N} \times \mathbf{I}_1 \cdot \boldsymbol{\omega}^{B/N} + \\ & \boldsymbol{\omega}^{B/N} \times (\mathbf{I}_2 \cdot (\boldsymbol{\omega}^{A/B} + \boldsymbol{\omega}^{B/N}) + \mathbf{h}) \end{aligned} \quad (6)$$

The assumption that the appendage is spherical eliminates the need to track the relative attitude of the two bodies here; \mathbf{I}_2 is constant in both B and A (and, in fact, in any frame). Also of interest is that equation (6) is closely related to the general equation of motion for a gyrost¹⁴. Such a model is typically used to describe the dynamics of dual-spin and momentum-bias satellites. Completing the governing equations requires

a description of the attitude kinematics, such as a differential equation in the direction-cosine matrix or in the Euler parameters. However, we note that none of the body-fixed torques depend on the inertial attitude; and, therefore, the attitude in N axes *per se* becomes irrelevant here.

The identities

$$\frac{B}{dt} \mathbf{h} + \boldsymbol{\omega}^{B/N} \times \mathbf{h} = \frac{A}{dt} \mathbf{h} + (\boldsymbol{\omega}^{A/B} + \boldsymbol{\omega}^{B/N}) \times \mathbf{h}. \quad (7)$$

and

$$\frac{B}{dt} (\boldsymbol{\omega}^{A/B} + \boldsymbol{\omega}^{B/N}) = \frac{A}{dt} \boldsymbol{\omega}^{A/B} + \frac{B}{dt} \boldsymbol{\omega}^{B/N}. \quad (8)$$

can be used to simplify the result somewhat. With the assumption that externally applied moments are zero and that the wheel momentum is constant in A ($\frac{A}{dt} \mathbf{h} = 0$), equation (6) becomes

$$\begin{aligned} 0 = & \mathbf{I}_1 \cdot \frac{B}{dt} \boldsymbol{\omega}^{B/N} + \boldsymbol{\omega}^{B/N} \times \mathbf{I}_1 \cdot \boldsymbol{\omega}^{B/N} + \\ & \mathbf{I}_2 \cdot \left(\frac{A}{dt} \boldsymbol{\omega}^{A/B} + \frac{B}{dt} \boldsymbol{\omega}^{B/N} \right) + \\ & \boldsymbol{\omega}^{B/N} \times \mathbf{I}_2 \cdot (\boldsymbol{\omega}^{A/B} + \boldsymbol{\omega}^{B/N}) + \\ & (\boldsymbol{\omega}^{A/B} + \boldsymbol{\omega}^{B/N}) \times \mathbf{h} \end{aligned} \quad (9)$$

Including the interface torque $\boldsymbol{\tau}$ represented by the 3DOF linear springs is arguably more intuitive if we assume small motions:

$$\boldsymbol{\tau} = \mathbf{c} \cdot \boldsymbol{\omega}^{A/B} + \mathbf{k} \cdot \boldsymbol{\theta}^{A/B} \quad (10)$$

where $\boldsymbol{\theta}^{A/B}$ is a vector of relative angular displacements that evolves from $\partial \boldsymbol{\theta}^{A/B} = \boldsymbol{\omega}^{A/B} \partial t$, and \mathbf{c} and \mathbf{k} are dyadics that represent viscous damping and spring stiffnesses, respectively. In the limit, all attitude representations approach this sort of small-angle approximation¹³. Now, thanks to the absence of internal forces, the two bodies interact only through $\boldsymbol{\tau}$.

$$\boldsymbol{\tau} = \mathbf{I}_1 \cdot \frac{B}{dt} \boldsymbol{\omega}^{B/N} + \boldsymbol{\omega}^{B/N} \times \mathbf{I}_1 \cdot \boldsymbol{\omega}^{B/N} \quad (11)$$

$$-\boldsymbol{\tau} = \mathbf{I}_2 \cdot \left(\frac{{}^A d}{dt} \boldsymbol{\omega}^{A/B} + \frac{{}^B d}{dt} \boldsymbol{\omega}^{B/N} \right) + \boldsymbol{\omega}^{B/N} \times (\boldsymbol{\omega}^{A/B} + \boldsymbol{\omega}^{B/N}) (\boldsymbol{\omega}^{A/B} + \boldsymbol{\omega}^{B/N}) \times \mathbf{h} \quad (12)$$

In order to achieve the objectives of this example we must apply techniques of linear algebra, which requires a matrix representation of the above vector-dyadic expressions. We use some orthonormal B-fixed basis vectors \mathbf{b}_i collected in a 1×3 vectrix $\mathbf{b} = [\mathbf{b}_1 \ \mathbf{b}_2 \ \mathbf{b}_3]$ such that, for example, equation (11) becomes

$$\mathbf{b} \begin{bmatrix} \tau_1 \\ \tau_2 \\ \tau_3 \end{bmatrix} = \mathbf{b} \mathbf{I}_1 \mathbf{b}^T \cdot \mathbf{b} \begin{bmatrix} \dot{\omega}_1^{B/N} \\ \dot{\omega}_2^{B/N} \\ \dot{\omega}_{31}^{B/N} \end{bmatrix} + \mathbf{b} \begin{bmatrix} 0 & -\omega_3^{B/N} & \omega_2^{B/N} \\ \omega_3^{B/N} & 0 & -\omega_1^{B/N} \\ -\omega_2^{B/N} & \omega_1^{B/N} & 0 \end{bmatrix} \mathbf{b}^T \cdot \mathbf{b} \mathbf{I}_1 \mathbf{b}^T \cdot \mathbf{b} \begin{bmatrix} \omega_1^{B/N} \\ \omega_2^{B/N} \\ \omega_{31}^{B/N} \end{bmatrix}, \quad (13)$$

where the inertia matrix I_1 is given by

$$I_1 = \begin{bmatrix} I_{11} & I_{12} & I_{13} \\ I_{12} & I_{22} & I_{23} \\ I_{13} & I_{23} & I_{33} \end{bmatrix} \quad (14)$$

Henceforth we will use the notation $\boldsymbol{\omega}^\times$ to represent the skew-symmetric matrix equivalent of the cross product, like the one that appears in equation (13). To linearize about a given gyroscopic condition, we allow that the angular velocity of the spacecraft may be nominally nonzero. We use $\boldsymbol{\omega}_0^{B/N}$ to represent this spinning condition. Let

$$\dot{\mathbf{x}} = \begin{bmatrix} \boldsymbol{\omega}^{B/N} \\ \boldsymbol{\omega}^{A/B} \end{bmatrix}. \quad (15)$$

Then

$$M\dot{\mathbf{x}} + C\dot{\mathbf{x}} + K\mathbf{x} = 0 \quad (16)$$

or

$$\dot{\mathbf{x}} + M^{-1}C\dot{\mathbf{x}} + M^{-1}K\mathbf{x} = 0, \quad (17)$$

where $M \in \mathfrak{R}^{6 \times 6}$, $C \in \mathfrak{R}^{6 \times 6}$, and $K \in \mathfrak{R}^{6 \times 6}$ are given by

$$M = \begin{bmatrix} I_1 & 0 \\ I_2 & I_2 \end{bmatrix}, \quad (18)$$

$$C = \begin{bmatrix} \omega_0^{B/N \times} I_1 - (I_1 \omega_0^{B/N})^\times & -c \\ \omega_0^{B/N \times} I_2 - (I_2 \omega_0^{B/N})^\times - h^\times & \omega_0^{B/N \times} I_2 - h^\times + c \end{bmatrix}, \quad (15)$$

and

$$K = \begin{bmatrix} 0 & -k \\ 0 & k \end{bmatrix}. \quad (19)$$

The asymmetry of this stiffness matrix is explained by our use of relative displacements for the motion of the appendage body but total displacements for the spacecraft body. In first-order form equation (17) yields a system dynamics matrix

$$A = \begin{bmatrix} 0 & 1 \\ M^{-1}K & -M^{-1}C \end{bmatrix}. \quad (20)$$

for M positive definite, which is always the case for physically realizable inertia matrices. A symmetric formulation that uses absolute displacements leads to a similar result, with

$$A = \begin{bmatrix} I_1^{-1}C & -I_1^{-1}C & I_1^{-1}K & -I_1^{-1}K \\ -I_2^{-1}(C+h^\times) & I_2^{-1}C & -I_2^{-1}K & I_2^{-1}K \\ 0 & 0 & -1 & 0 \\ 0 & 0 & 0 & -1 \end{bmatrix}. \quad (21)$$

There are three zero eigenvalues, corresponding to rigid-body spinning configurations of the entire system, related to the so-called relative equilibria^{1,15} for the complete nonlinear solution for a gyrost. In an effort to illustrate the remaining eigenvalues, we provide a root locus for the eigenvalues of the system as the magnitude of h varies. In this example, we choose $I_1 = [[300 \ -4 \ 5]^T \ [-4 \ 400 \ -3]^T \ [5 \ -3 \ 500]^T]$, $h \parallel [1 \ 1 \ 1]^T$ (the magnitude varies), $k = \text{diag}(100 \ 200 \ 300)$, $c = \text{diag}(100 \ 100 \ 100)$, $I_2 = 100$, and $\omega_0^{B/N} = 0$. Figure 3 shows the variation in modal frequency as the gyricity increases, and Figure 4 shows how modal damping changes. Figure 5 is a root locus for the same system showing the behavior of the eigenvalues in the real-imaginary plane. Figures 6 and 7 show these behaviors for an identical system but with no viscous damping ($c=0$).

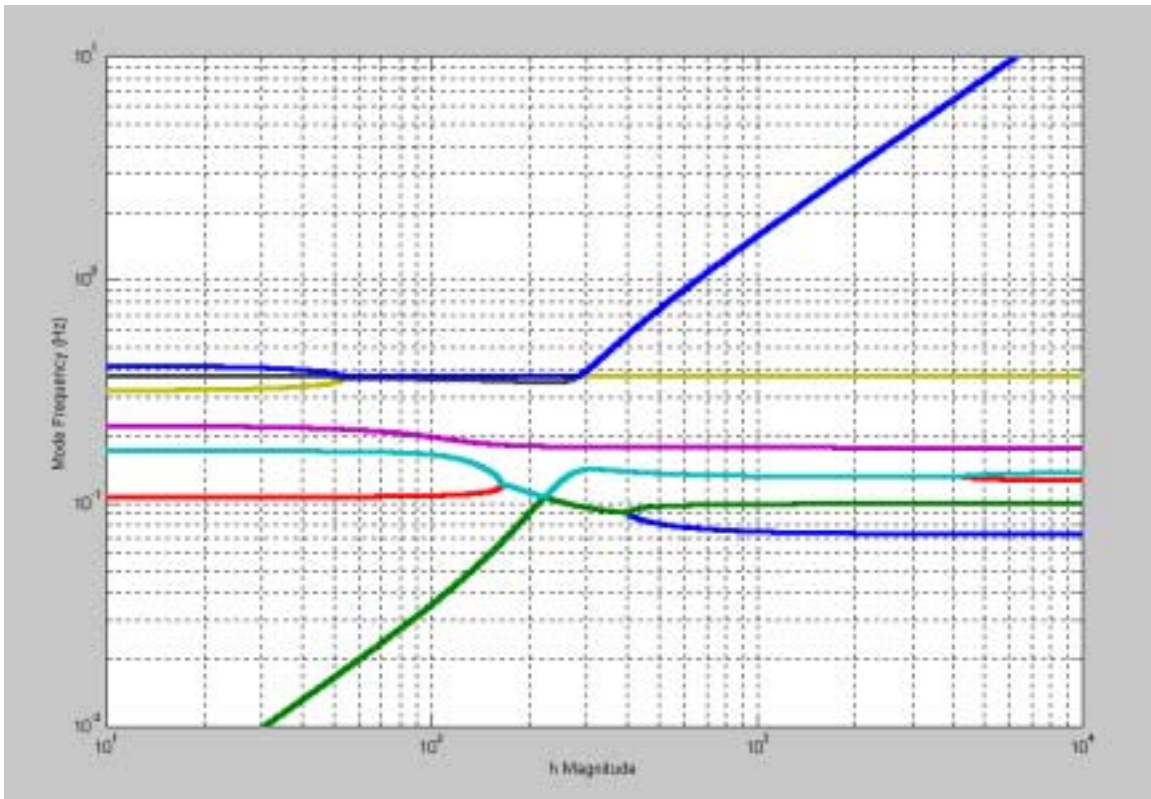


Figure 3. Frequency Shift Due to Gyricity for $c=100$.

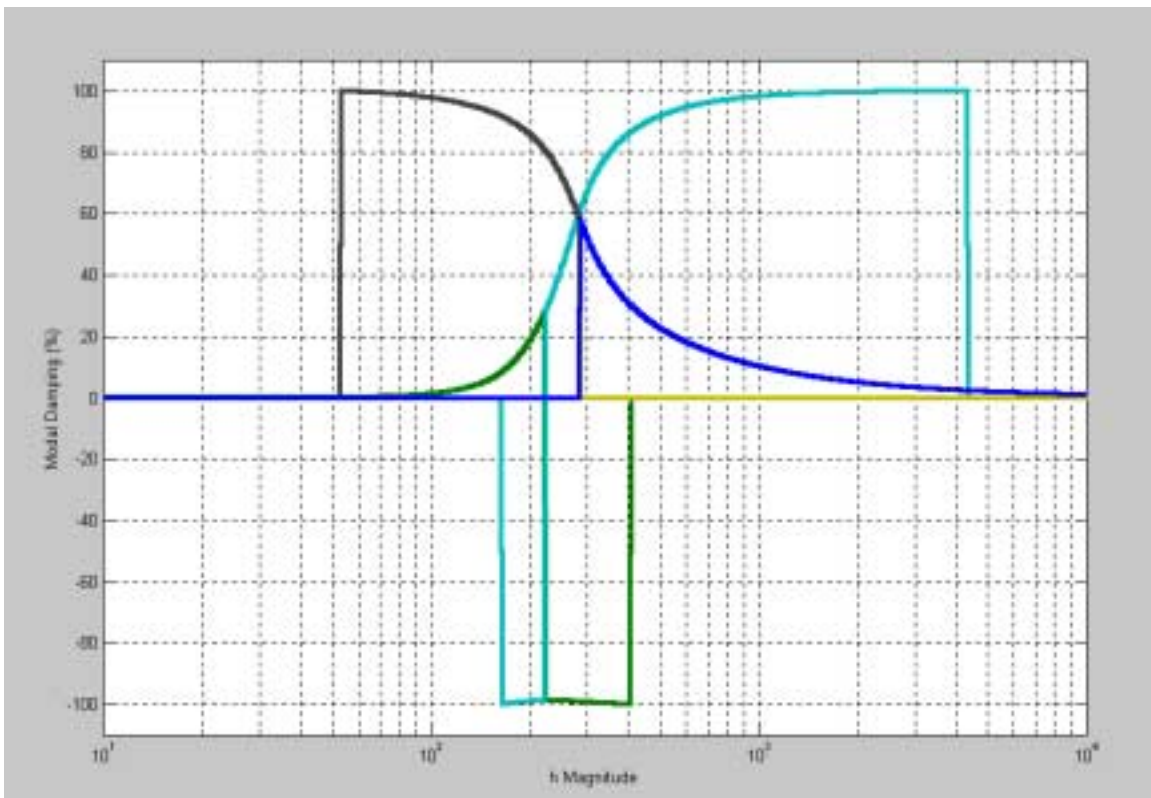


Figure 4. Damping Shift Due to Gyricity for $c=100$.

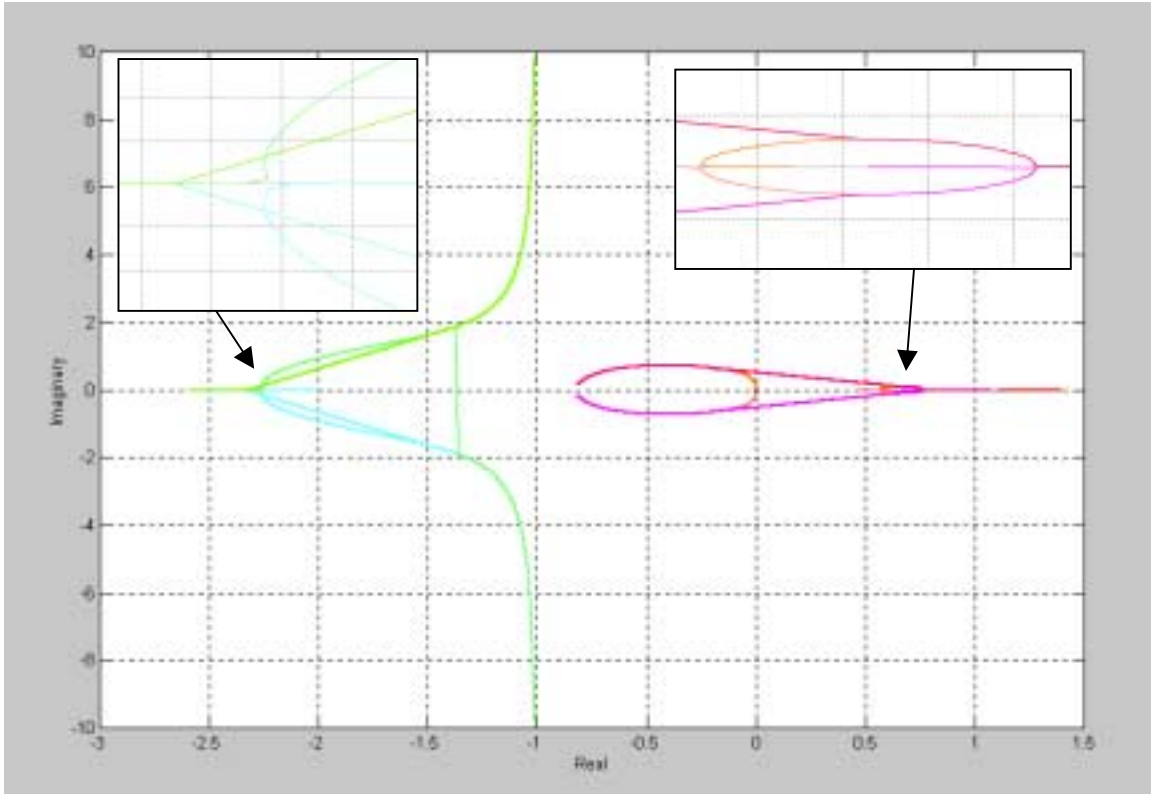


Figure 5. Root Locus for $c=100$.

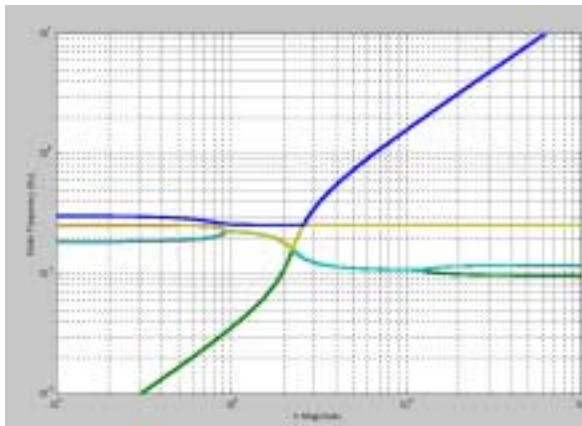


Figure 6. Frequency Shift Due to Gyricity for $c=0$.

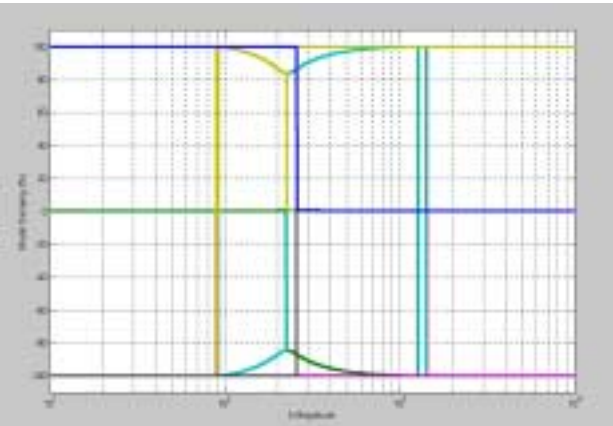


Figure 7. Frequency Shift Due to Gyricity for $c=0$.

In the case of the example shown above, several features of the proposed concept are clear. First, it is evident that the frequencies shift both up and down due to a bifurcation, as predicted in D'Eleuterio's work. Also, the presence of the angular momentum can cause significant coupling among modes. This feature is evident in the middle of the range of h variation, where two modes that are distinct without the added momentum coalesce when the momentum becomes significant. This coupling can be exploited to improve observability and/or controllability¹⁰. Another important

feature is that clearly the angular momentum effectively stiffens (or reduces the effective modal mass) of at least some modes. The stiffening appears throughout the root locus, which shows various modes increasing and decreasing in frequency as the momentum increases. Furthermore, even in the case of zero viscous damping, momentum augmentation introduces changes in the real parts of the eigenvalues. Taking advantage of these bifurcations requires some knowledge of the parameters of the system so that enough (and not too much) momentum can be introduced for the desired effect.

CONCLUSION: SYSTEMS ENGINEERING WITH EMBEDDED MOMENTUM

Adjusting the structural response with gyricity may take several forms. One approach is to use a single, or relatively few, discrete actuators so that the gross behavior of the first few modes of a structure can be adjusted. Another is to distribute gyricity throughout a structure with small enough actuators that the gyroscopic elements can be modeled as a continuum.

Weight and cost are important considerations in any such enterprise, and the benefits offered by embedded momentum must somehow exceed the weight savings of leaving the structure unaugmented. Table 1 lists some state-of-the-art momentum actuators and suggests possible uses in structural adaptation with this principle in mind.

Table 1. Momentum Actuators

Momentum Actuator	Momentum Density (Nms/kg)	NASA Technology Readiness Level (TRL 1 - 9)	Gyroelastic Use
Traditional CMGs	2.0 - 15	9	Medium-precision, high-inertia structures that may benefit from active compensation
M50 CMG	0.9 - 2.7	6	
Constellation Reaction Wheels	2.0 - 17	9	Structures with little room for mass growth and that require compensation of only a few fundamental modes
HR0610 Reaction Wheels	1.1 - 2.4	9	Structures with some room for mass growth and that require compensation of only a few fundamental modes
Silicon Microwheels	9	4	Structures whose adaptation requires gyroelastic continua

The silicon microwheels described in Table 1 offer a high momentum density¹⁶. They are a few inches across and are predicted to consume less than 1W of power. They are among very few technologies available for implementing structural adaptation via gyroelastic continua. A similar, but less dense device is Honeywell's HR04 reaction wheel: 0.2 to 1.0 Nms at about 1.2 kg. CMGs are used in place of reaction wheels when very high torques are required. Our discussion does not preclude their use, but we have focused on constant-momentum designs, which would be tuned once and left alone. Momentum wheels would be appropriate for establishing a fixed deformation in an appendage of a spinning spacecraft, while the torque capability of a CMG for this application would be

wasted. Active actuation of structures via an array of CMGs would likely be very efficient, but to date the smallest available CMG design is the 25-75 Nms M50 shown. Wheels like the constellation-series reaction wheels offer the highest momentum density, and from a weight standpoint, are likely to be among the best technologically mature choices for space structures.

For all of these momentum actuators, the spacecraft's jitter response must be considered. For this reason, gyric compensation of a finely pointed antenna or optical instrument is probably ill advised unless active magnetic bearings or a similar advanced suspension technology are incorporated. In the case of most magnetic bearings, which (by Earnshaw's theorem) require active control for stability, power consumption is likely to be the driving issue.

APPENDIX: MODELING NONLINEAR GYROELASTIC SYSTEMS WITH LINEAR FINITE-ELEMENT MODELS

While there have been many approaches to modeling the coupled dynamics of flexible structures and gyroscopics, the following method proposed by Richard I. McMonagle in 1998 has proven to be both elegant and complete¹⁷. Furthermore, it can use finite-element models (such as NASTRAN) by reinterpreting the gridpoint displacements as path-length variables and tracking them through individual-element coordinate-system rotations.

Traditional finite element methods take the familiar form:

$$M\ddot{x} + C\dot{x} + Kx = F_{\text{applied}} \quad (\text{A.1})$$

While simple and easy to implement, this form neglects nonlinear terms, and in interpreting displacements in an inertial frame, fails to produce accurate results for large angle motions like spacecraft spin dynamics. McMonagle's method augments the applied force F with a vector of element gyroscopic forces so that for each element

$$F \Rightarrow m(\ddot{x} + \omega \times \dot{x}) \quad (\text{A.2}),$$

using only the displacement variables from the finite-element grid points. Transforming an $n \times n$ system of linear finite-element equations of motion to normal form with n generalized coordinates q via $x = \Phi q$ yields

$$\ddot{q} + 2\zeta_m \omega_m \dot{q} + \omega_m^2 q = \Phi^T (F_{\text{applied}} + F_{\text{gyro}}), \quad (\text{A.3})$$

where ω_m is a diagonal matrix of modal frequencies with ζ as the modal damping ratio, and Φ contains the eigenvectors. This form is exactly the same as the standard normal-modes form with only the addition of F_{gyro} . The final equation in normal mode form used in numerical integration for an n -DOF system is

$$\ddot{q} + 2\zeta\omega_m\dot{q} + \omega_m^2 q = \Phi^T F_{applied} + E \begin{Bmatrix} \dot{q}_1 \dot{q} \\ \dot{q}_2 \dot{q} \\ \dots \\ \dot{q}_n \dot{q} \end{Bmatrix}, \quad (A.4)$$

where E is a time-invariant matrix of system parameters that can be found through algebraic manipulation of

$$E \begin{Bmatrix} \dot{q}_1 \dot{q} \\ \dot{q}_2 \dot{q} \\ \dots \\ \dot{q}_n \dot{q} \end{Bmatrix} \equiv -\Phi^T \begin{Bmatrix} M_{transgrid1} \omega_{grid1} \times \dot{x}_{grid1} \\ \omega_{grid1} \times M_{rotationlg rid1} \omega_{grid1} \\ M_{transgrid2} \omega_{grid2} \times \dot{x}_{grid2} \\ \omega_{grid2} \times M_{rotationlg rid2} \omega_{grid2} \\ \vdots \\ \vdots \\ M_{transgridn} \omega_{gridn} \times \dot{x}_{gridn} \\ \omega_{gridn} \times M_{rotationlg ridn} \omega_{gridn} \end{Bmatrix} \quad (A.5)$$

Incorporating holonomic and non-holonomic constraints for jointed bodies can be accomplished with a number of different formulations, although the Udwadia-Kalaba approach¹⁸ has been shown to be very versatile for simulations with McMonagle's method.

REFERENCES

[1] J. N. Juang and M. J. Balas, "Dynamics and Control of Large Spinning Spacecraft," *The Journal of the Astronautical Sciences*, Vol. XXVIII, No. 1, January-March, 1980, pp. 31-48.

[2] R. E. Zee and G. R. Heppler, "Dynamics of Gyroelastic Beams," in Proceedings of the 35th AIAA/ASME/ASCE/AHS/ASC Structures, Structural Dynamics and Materials Conference, AIAA/ASME Adaptive Structures Forum, Vol. 2, 1994 Hilton Head, SC pp. 1048-1057.

[3] O.Song, H.D.Kwon and L.Librescu, "Bending Vibration of Gyroelastic Beams Incorporating Adaptive Capabilities," AIAA-98-2041, 39th AIAA SDM Conference, LA, CA, USA, April 1998.

[4] K. Yamanaka, G. R. Heppler and K. Huseyin, "Stability of Gyroelastic Beams," *AIAA Journal*, Vol. 34, No. 6, June 1996, pp 1270-1278.

[5] G. M. T. D'Eleuterio, "Dynamics and Control of Gyro-Elastic Space Vehicles," Ph.D. Dissertation, University of Toronto, Institute for Aerospace Studies, 1983.

[6] G. M. T. D'Eleuterio and P. C. Hughes, "Dynamics of Gyroelastic Continua," *Journal of Applied Mechanics*, Vol. 51, 1984, pp. 415-422.

[7] P. C. Hughes and G. M. T. D'Eleuterio, "Modal Parameter Analysis of Gyroelastic Continua," *Journal of Applied Mechanics*, Vol. 53, 1986, pp. 918-924.

[8] G. M. T. D'Eleuterio, "On the Theory of Gyroelasticity," *Journal of Applied Mechanics*, Vol. 55, 1988, pp. 488-489.

[9] C. J. Damaren and G. M. T. D'Eleuterio, "Optimal Control of Large Space Structures Using Distributed Gyricity," *AIAA Journal of Guidance, Control, and Dynamics*, Vol. 12, No. 5, Sept.-Oct. 1989, pp. 723-731.

[10] C. J. Damaren and G. M. T. D'Eleuterio, "Controllability and Observability of Gyroelastic Vehicles," *AIAA Journal of Guidance, Control, and Dynamics*, Vol 14, No. 5, Sept.-Oct. 1991, pp. 886-894.

[11] G. M. T. D'Eleuterio and P. C. Hughes, "Dynamics of Gyroelastic Spacecraft," *AIAA Journal of Guidance, Control, and Dynamics*, Vol. 10, No. 4, July-August, 1987. pp. 415-422.

[12] Hughes, P. C., *Spacecraft Attitude Dynamics*, John Wiley and Sons, New York, 1986.

[13] M. Peck, "Stable Relative Equilibria of a Dissipative Controller for Gyrostat Attitude," Proceedings of the 2001 AAS Astrodynamics Specialist Conference, Quebec City, Canada; July 2001

[14] M. Peck, "Stable Relative Equilibria of a Dissipative Controller for Gyrostat Attitude," Proceedings of the 2001 AAS Astrodynamics Specialist Conference, Quebec City, Canada; July 2001.

[15] C. Hall, "Relative Equilibria of a Gyrostat," *Journal of Guidance, Control, and Dynamics*, Vol. 20, July-Aug. 1997, pp. 625-632.

[16] A. Peczalski, D. Youngner, and H. B. French, "Microwheels for Attitude Control and Energy Storage in Small Satellites" Proceedings of the IEEE Aerospace 2001 Conference, Big Sky, Montana, 10-17 March 2001, Vol. 5, pp. 2483-2492.

[17] R. I. McMonagle, M.S. Thesis, University of Southern California, 1998.

¹⁸ F. E. Udwadia and R. E. Kalaba, *Analytical Dynamics: A New Approach*, Cambridge University Press, 1996.